Molecular Cell, Vol. 6, 803–814, October, 2000, Copyright ©2000 by Cell Press

Analysis of the Okazaki Fragment Distributions along Single Long DNAs Replicated by the Bacteriophage T4 Proteins

Paul D. Chastain II,* Alexander M. Makhov,* Nancy G. Nossal,† and Jack D. Griffith*‡
*Lineberger Comprehensive Cancer Center
University of North Carolina at Chapel Hill
Chapel Hill, North Carolina 27599
†Laboratory of Molecular and Cellular Biology
National Institute of Diabetes
and Digestive and Kidney Diseases
National Institutes of Health
Bethesda, Maryland 20892

Summary

Rolling circle replication from M13 DNA circles was previously reconstituted in vitro using purified factors encoded by bacteriophage T4. The products are duplex circles with linear tails >100 kb. When T4 DNA polymerase deficient in 3′ to 5′ exonuclease activity was employed, electron microscopy revealed short single-stranded DNA "flaps" along the replicated tails. This marked the beginning of each Okazaki fragment, allowing an analysis of the lengths of sequential Okazaki fragments on individual replicating molecules. DNAs containing runs of Okazaki fragments of similar length were found, but most showed large length variations over runs of six or more fragments reflecting the broad population distribution.

Introduction

The coordinated replication of DNA involves many proteins working in unison in a single complex termed the replisome (reviewed in Kornberg and Baker, 1992). A central role of the replisome is ensuring that both the leading and lagging strands are replicated at the same net rate. This is accomplished by continuous 5′ to 3′ synthesis on the leading strand template and discontinuous synthesis in the same enzymatic (but opposite physical) direction on the lagging strand. After the RNA primers are removed from the lagging strand fragments (Okazaki fragments), the gaps are repaired by polymerase and the fragments joined by DNA ligase. The coupling of leading and lagging strand replication in the several systems examined is facilitated by a dimeric polymerase assembly, one polymerase replicating the leading strand and the other replicating the lagging strand (Wu et al., 1992c; Stukenberg et al., 1994; Yuzhakov et al., 1996; Salinas and Benkovic, 2000). Since sites of synthesis on the leading and lagging strands may be separated by up to several thousand base pairs, it was proposed that a portion of the lagging strand loops back to allow the lagging strand polymerase to be tethered to the replisome (Sinha et al., 1980; Alberts et al., 1983). The loops would thus grow and collapse with each cycle of Okazaki fragment synthesis. Recent electron microscopic (EM) studies using purified T7 proteins have visualized these loops (Lee et al., 1998; Park et al., 1998).

The range of Okazaki fragment sizes produced by the different prokaryotic replication systems is surprisingly similar in spite of very different templates and replication proteins. In *E. coli*, Okazaki fragments average between 1000–2000 nt in vivo, consistent with in vitro studies using purified proteins and M13 DNA templates (Wu et al., 1992a, 1992b, 1992c; Zechner et al., 1992a, 1992b). Similar lengths are found when M13 templates are replicated by purified T4 phage proteins (Alberts et al., 1983; Selik et al., 1987). Studies with bacteriophage T7 proteins and M13 DNA templates have shown that Okazaki fragments average ~2300 nt (Debyser et al., 1994; Park et al., 1998), and reducing the size of the template circle 100-fold to 70 bp does not change the average Okazaki fragment length (Lee et al., 1998). The T4 proteins have recently been shown to produce fragments of similar size on these small 70 bp circular templates (Salinas and Benkovic, 2000). Variations in the mean Okazaki fragment size can be forced. Using the purified T4 proteins, Selik et al. (1987) found that limiting the ribonucleotide concentration increased the mean Okazaki fragment size from 1200 nt to 6000 nt. Dilution of the T7 primase/helicase (Park et al., 1998) or the *E. coli* primase (Wu et al., 1992a, 1992b, 1992c; Zechner et al., 1992a, 1992b) in vitro generated small but measurable shifts in the mean fragment size.

Okazaki fragments are extended from RNA primers laid down by primase. The availability of priming sites, however, does not appear to control fragment length. For T4 primase, the recognition sequences are 3′-TTG-5′ and 3′-TCG-5′ on unmodified DNA but only 3′-TTG-5′ on T4 DNA, which contains hydroxymethylcytosine in place of cytosine (Hinton and Nossal, 1987). These recognition sequences occur, on average, every 14 bp for M13 and 50–60 bp for T4 phage templates (Selik et al., 1987). Two T7 priming sites are present in the 70 bp mini circle template, yet a new Okazaki fragment is initiated only once every ~20 circuits of the template DNA (Lee et al., 1998). Several models have been proposed to explain the initiation of Okazaki fragments.

Models based on the T4 studies of Alberts and coworkers (collision models) suggest that a new fragment is initiated when the lagging strand polymerase collides with the 5′ terminus of the previous fragment (Alberts et al., 1983; Nossal and Alberts, 1983; Selik et al., 1987; Richardson and Nossal, 1989; Richardson et al., 1990; Nossal, 1994). Marians and coworkers proposed a "primase control model" in which synthesis of the primer for the next Okazaki fragment serves as the signal for the lagging strand polymerase to disengage from the previous Okazaki fragment (Wu et al., 1992a, 1992b, 1992c; Zechner et al., 1992a, 1992b; Tougu and Marians, 1996). In the collision model, the length of each Okazaki was originally thought to reflect the size of the initial fragment synthesized (Alberts et al., 1983). However,

‡To whom correspondence should be addressed (e-mail: jdg@med.unc.edu).

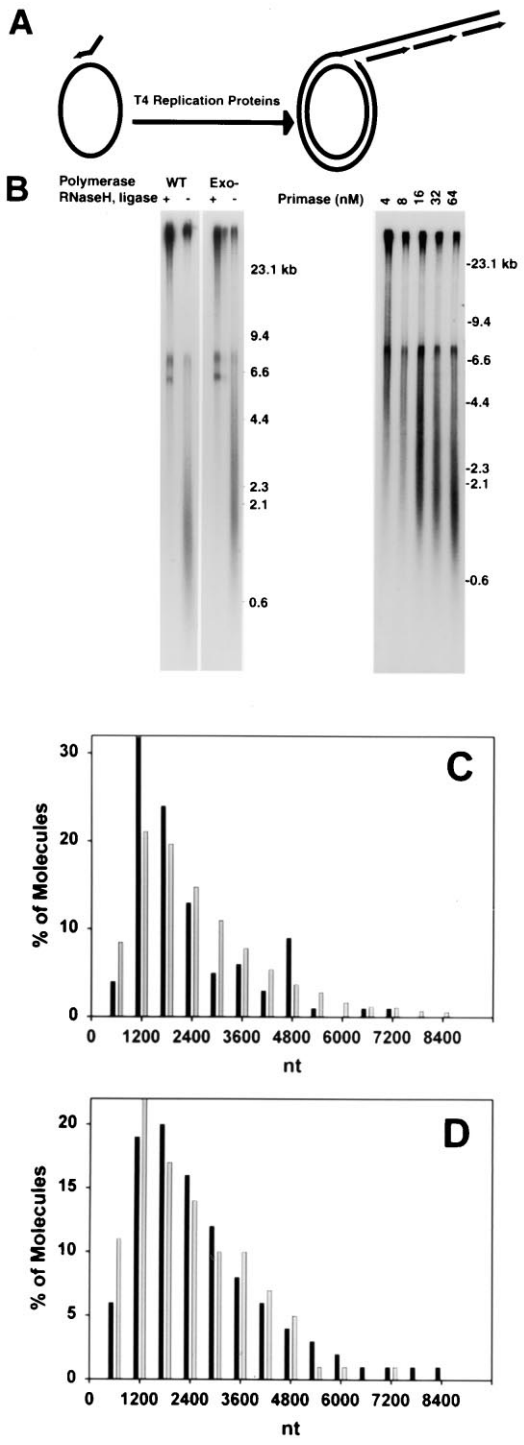

Figure 1. Comparison of Replication Products Generated by Wild-Type and D219A Mutant Polymerases

(A) The template used in these studies (Nossal et al., 1995) consists of M13mp2 ssDNA to which an 84 nt oligonucleotide is annealed. The first 34 nt from the 3′ end of the oligonucleotide are complementary to M13 mp2 ssDNA, while the remaining 50 nt are not. The 3′ terminus of this primer is extended by the T4 replication proteins to initiate rolling circle replication.

(B) Rolling circle replication reactions were carried out at 37°C for 5 min using the template in (A) and the following T4 replication proteins: genes 44/62 clamp-loader, gene 45 polymerase clamp, 32 protein, gene 61 primase, gene 41 helicase, gene 59 helicase loading protein, and wild-type or D219A mutant T4 DNA polymerase. Samples were loaded onto alkaline agarose gels, and the DNA products were separated by electrophoresis (see Experimental Procedures). Molecular weights were derived from marker lanes (not shown). In the reactions without T4 RNase H and DNA ligase, the sharp band near 7200 nt is the product of molecules on which synthesis stopped after the M13 ssDNA was copied. The smeared shorter DNA is from Okazaki fragments. In the reactions with RNase H and DNA ligase, the band running below the 6.6 kb marker is denatured closed circular duplex DNA. The reactions for the gel on the left included primase at 64 nM. The reactions for the gel on the right contained primase at the indicated concentrations and lacked RNase H and ligase.

(C and D) Comparison of the distribution of Okazaki fragment sizes determined by alkaline agarose gel electrophoresis (light bars) or EM measurement (dark bars). In (C), the reaction was catalyzed by the D219A mutant DNA polymerase in the absence of RNase H and DNA ligase, and in (D), the reaction was catalyzed by wild-type DNA polymerase with RNase H and DNA ligase. Measurement of the fragment lengths by EM is described in the text. Fragment lengths from the alkaline gels (as in [B]) were reduced to number average distributions and further sliced into histograms to mimic the EM data as described in Experimental Procedures and the text. In the absence of RNase H and ligase (C), all Okazaki fragments are compared, while in (D) only the most recently synthesized fragments are compared.

Selik et al. (1987) later suggested that the Okazaki fragment "measuring stick" is not necessarily the first fragment, but rather the fragment made when the replication system has reached equilibrium, determined by the relative rates of leading and lagging synthesis and the time between completion of a lagging strand fragment and release of the lagging strand polymerase. At this point, all subsequent Okazaki fragments would be roughly of similar size as long as the system remained in equilibrium.

In the primase control model, the size of an Okazaki fragment depends primarily on the efficiency with which primase binds to the helicase and synthesizes primers (Tougu and Marians, 1996). It would also be influenced by how quickly the lagging strand polymerase disengages from its current Okazaki fragment and initiates synthesis of the next fragment. In this model, if primase and nucleotide concentrations do not change, the size of any Okazaki fragment relative to its neighbor should be similar.

Both models predict that along a single molecule undergoing replication, the Okazaki fragments synthesized at equilibrium should have a relatively narrow size distribution. This, however, does not appear to be the case, based on the broad distribution of fragment sizes observed on alkaline gels. The distribution of fragment lengths for any given replicating molecule may be narrow, with each single molecule distribution differing markedly from the next, such that collectively they generate the broad distribution observed experimentally. Alternatively, (not as easily explained by these models) the distribution along single replicating molecules might be found to be broad and similar to that of the population.

Wild-type T4 DNA polymerase copying a single-stranded DNA template is released rapidly when it reaches duplex DNA (Hacker and Alberts, 1994). In contrast, the exonuclease-defective mutant polymerase

D219A (Frey et al., 1993) continues synthesis for a short distance when it reaches an annealed fragment, displacing a segment of the 5′ terminus, creating a single-stranded DNA flap (M. Bhagwat and N. G. N., submitted). Examination of the products of rolling circle synthesis by this D219A T4 polymerase revealed the expected flaps along the long rolling circle tail when the flaps were stained with a single strand binding (SSB) protein. Their location along the rolling circle tail thus flagged the junctions between adjacent Okazaki fragments and provided a means of analyzing the lengths of successive fragments along single replicating DNAs. This report describes the results of a detailed analysis of these fragment distributions.

Results

Visualization of Rolling Circle Intermediates Using an Exonuclease-Deficient Polymerase

To visualize the junctions between adjacent Okazaki fragments, we carried out rolling circle synthesis with T4 replication proteins, using the exonuclease-defective (D219A) T4 DNA polymerase. We expected to see single-stranded flaps at these junctions because this mutant polymerase continues synthesis for a short distance when it reaches an annealed fragment ahead (see Introduction). M13 ssDNA annealed to an 84 nt oligomer was used as a template. The 34 nt complementary portion of the oligonucleotide serves as a primer for the replication of the M13 ssDNA template, and the 50 nt noncomplementary portion serves as a site from which rolling circle replication is initiated after the ssDNA template is replicated (Figure 1A). Replication is catalyzed by T4 DNA polymerase, a trimeric gene 45 sliding clamp, the clamp loading system (gene 44/62 complex), gene 32 single strand binding protein, gene 41 helicase, gene 59 helicase loading protein and gene 61 primase (reviewed in Nossal, 1994). The RNA primers (predominantly pppApCpNpNpN) that begin the lagging strand fragments and a short region of the adjacent DNA are removed by T4 RNase H, a 5′ nuclease that degrades both the RNA·RNA and DNA·DNA duplexes; the gaps are repaired by DNA polymerase and the nicks sealed by T4 DNA ligase (Hollingsworth and Nossal, 1991; M. Bhagwat and N. G. N., submitted).

Alkaline gel analysis of the T4 replication products generated in the absence of RNase H and DNA ligase revealed two distinct populations of DNA products (Figure 1B). Products with lengths greater than 23 kb are the result of leading strand synthesis. The broad band of shorter products consists mostly of individual lagging stand fragments, observed only in reactions with primase, and some stalled, incomplete leading strands present even without primase. The distribution of lagging strand products with the wild-type polymerase is shifted slightly to shorter fragment lengths relative to that with the D219A polymerase for two reasons. First, when RNase H and DNA ligase are omitted from the wild-type polymerase reaction, the exonuclease activity of the polymerase leads to some degradation of the 3′ termini of at least half of the fragments. The resulting ssDNA gaps were observed by EM as described below.

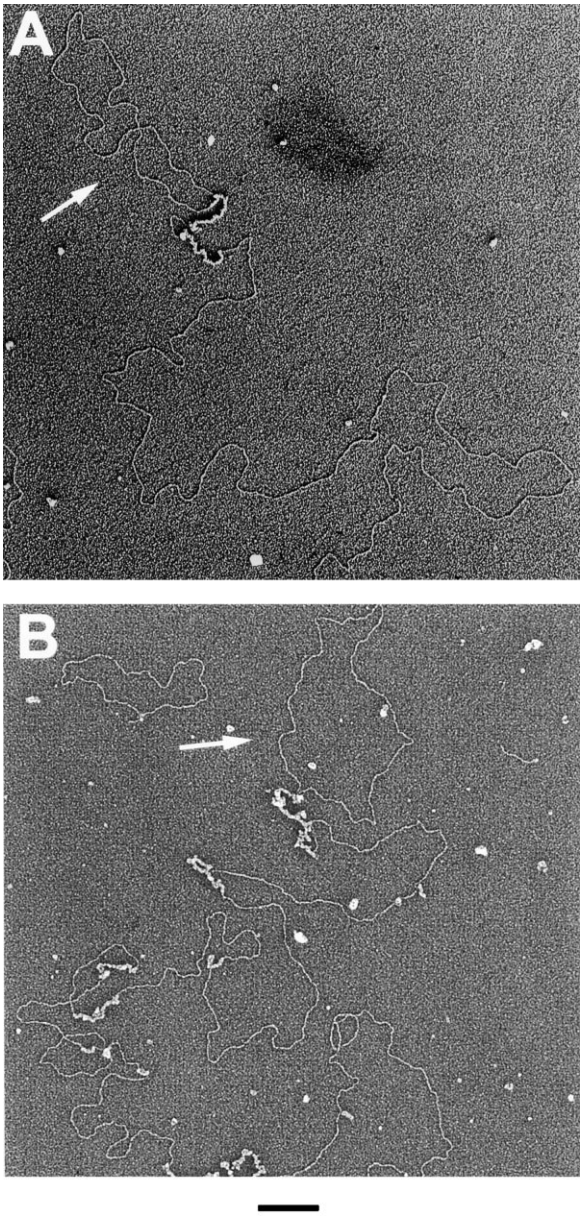

Figure 2. Visualization of Replication Products Catalyzed by Wild-Type T4 DNA Polymerase

Rolling circle replication reactions were carried out as described in Figure 1 using wild-type T4 DNA polymerase with (A) or without (B) RNase H and DNA ligase. Following incubation for 5 min, the samples were deproteinized, and the single-stranded segments were complexed with *E. coli* SSB protein to generate thick extended segments, as contrasted to the thin duplex DNA. The samples were then fixed by glutaraldehyde and directly prepared for EM, including mounting on thin carbon foils, washing, and rotary shadowcasting with tungsten. The long tracts of ssDNA in (B) are the result of exonucleolytic degradation by wild-type DNA polymerase. Arrows indicate the M13 template circles. Shown in reverse contrast, bar equals a length of dsDNA equivalent to 1.1 kb (A) or 1.0 kb (B).

Second, the fragments generated by the D219A polymerase are lengthened when the polymerase displaces the fragment ahead. When RNase H and DNA ligase are present, most of the lagging strand fragments are sealed to form strands longer than 23 kb, which migrate with

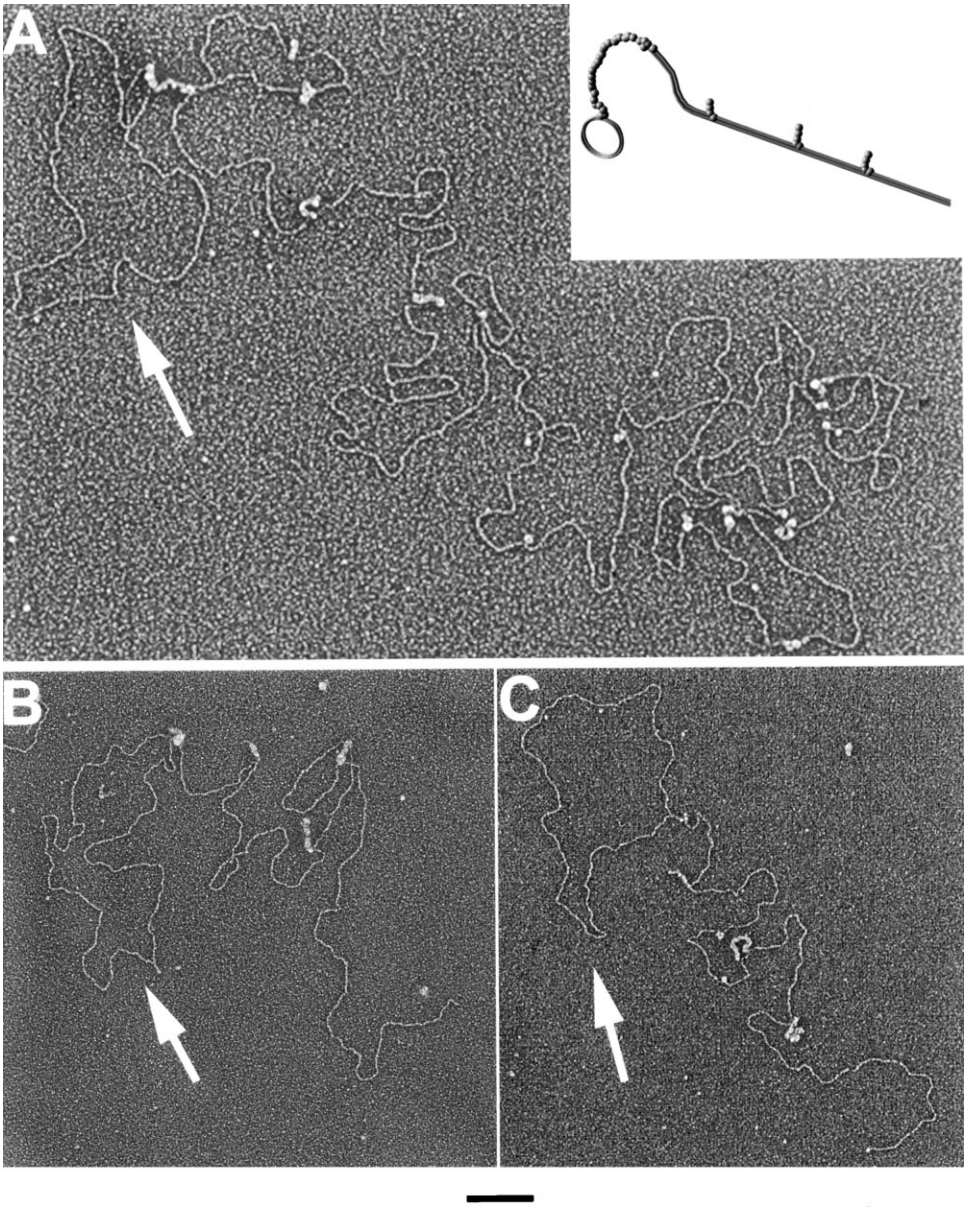

Figure 3. Visualization of Replication Products Catalyzed by D219A T4 DNA Polymerase

Rolling circle replication reactions were carried out as described in Figures 1 and 2 using D219A T4 DNA polymerase without RNase H and DNA ligase. Following incubation for 5 min, the samples were deproteinized and prepared for EM as described in Figure 2. Arrows indicate the M13 template circles. Because of the strand invasion properties of the D219A mutant polymerase, ssDNA flaps were expected to be generated at the junction of each completed Okazaki fragment (inset). Primase was present at 64 nM (A and B) or 8 nM (C). There are 23 Okazaki fragments in A, 4 in B, and 6 in C. The SSB-stained flaps tend to be longer with reduced primase (C). Shown in reverse contrast, bar equals a length of dsDNA equivalent to 1.1 kb (A), 1.0 kb (B), or 0.8 kb (C).

the leading strand products (Figure 1B). There is a band running below the 6.6 kb marker that is denatured closed circular duplex.

Other than generating short, single-stranded flaps at the junctions of the Okazaki fragments, the D219A polymerase was found to behave like the wild-type polymerase. Synthesis occurs at 400 nt per second at 30°C for both enzymes, and the final extent of replication is the same, with linear tails of multiple unit length being produced (data not shown, see also Salinas and Benkovic, 2000). Alkaline gel analysis of the Okazaki fragments shows a broad distribution from 500 to 4400 nt under optimal conditions with 64 nM primase (Figure 1B, left). The mutant polymerase provided an additional advantage for the EM analysis in that it cannot degrade the 3′ termini of the Okazaki fragments following their synthesis.

To visualize the ssDNA segments along the length of the rolling circle tails, the samples were deproteinized and incubated with *E. coli* SSB protein that binds ssDNA to generate a thick, stiff filament easily distinguished from double-stranded DNA (dsDNA) and that is 1.8 times

shorter than the equivalent duplex length. The samples were prepared for EM (see Experimental Procedures).

Inspection of DNA molecules taken from reactions containing the wild-type T4 replication proteins including RNase H and DNA ligase revealed M13 duplex circles with linear double-stranded tails, some of which were greater than 100 kb. The fraction of circles that contained tails varied from 50% to 70% (n = 1000 in 10 different experiments). At the junction of the tail and the M13 circle, three different DNA arrangements were observed. In some molecules, the duplex DNA tail was joined to the circle by a single segment of ssDNA stained by SSB (43%). In others (31%), there were two SSB-stained ssDNA segments (Figure 2A), one at the tail-circle junction and a second one usually within 1–2 kb downstream on the tail. Finally, in others (26%), there were multiple ssDNA regions stained by SSB, one at the tail-circle junction, and the rest located within 5–10 kb downstream on the tail. Molecules without any SSB-stained regions were not found. These three forms have been described before (Park et al., 1998). Molecules with one ssDNA segment represent examples in which the last Okazaki fragment has been completed, and in which helicase moving on the lagging strand is unwinding the duplex at the fork. Molecules with two ssDNA segments represent molecules in which duplex unwinding is occurring concomitant with synthesis of an Okazaki fragment. Finally, molecules with more than two ssDNA segments represent molecules that possess multiple incomplete Okazaki fragments.

When T4 RNase H and DNA ligase were omitted from the synthesis reactions (containing the wild-type polymerase), the long rolling circle tails showed ssDNA segments stained by SSB scattered along the full length of the tail (Figure 2B). The ssDNA gaps were not placed evenly throughout the dsDNA tail as would be the case if the 3′ terminus of each Okazaki fragment had undergone limited 3′ to 5′ degradation. Rather, some termini appeared to have been spared (Figure 2B), as the length of some dsDNA segments was greater than 14 kb, while in others the ssDNA gaps were greater than 6 kb, suggesting that one or more adjacent Okazaki fragment had been fully degraded (Figure 2B). The longest duplex length in Figure 2B is 9 kb, and the longest ssDNA length is 4 kb.

When reactions without T4 RNase H and DNA ligase were carried out with D219A DNA polymerase, the products were duplex circles, many with long linear tails (50%–70% of the circles). Along the tails were thick stubs or flaps consisting of short segments of ssDNA stained by SSB extending out from the tail (Figures 3A and 3B). These flaps were never observed along the M13 circle, showing that the D219A polymerase cannot introduce flaps along continuous duplex DNA.

Measurement of Okazaki Fragment Lengths: Comparison of Alkaline Gel and EM Values

Two classes of Okazaki fragments were analyzed. The first set were nascent fragments in the process of being synthesized, and the other set were ones that had been completed (Figures 4A and 4B, respectively). For this analysis, a nascent Okazaki fragment is defined as beginning at the start of the first duplex region after the template-replication tail junction, continuing toward the distal end of the tail through the duplex segment, and ending at the far end of the adjoining ssDNA gap (Figure 4A). This definition is based upon the assumption that continued synthesis of the dsDNA segment by the lagging strand polymerase would have filled in the abutting ssDNA gap. Nascent fragments can be observed in reactions with or without T4 RNase H and DNA ligase and with the wild-type and D219A mutant polymerase. An analysis of such fragments using this definition was carried out in the T7 system in Park et al. (1998).

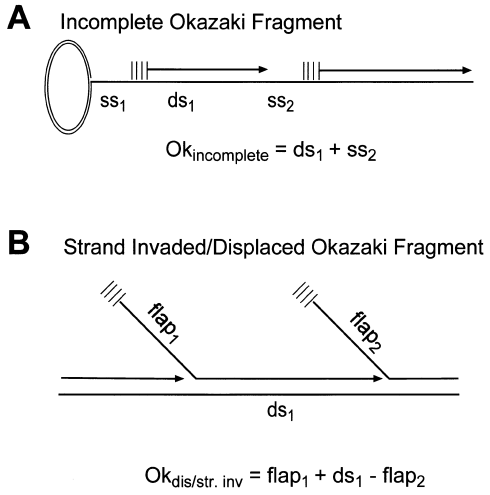

Figure 4. Determining the Length of Okazaki Fragments by EM

(A) An Okazaki fragment in the process of synthesis consists of two segments, a duplex region (ds_1) and a single-stranded region (ss_2). The former corresponds to the amount of lagging strand synthesis that has occurred, and the latter corresponds to the remaining template to be synthesized.

(B) A completed Okazaki fragment produced by the D219A mutant polymerase in the absence of RNase H and ligase consists of three segments, a displaced region ($flap_1$), a duplex region (ds_1), and a flap generated by strand invasion into the next fragment ($flap_2$). $Flap_1$ corresponds to the amount of DNA displaced by the D219A mutant polymerase while synthesizing the next, more recent, Okazaki fragment. The ds_1 segment corresponds to the duplex portion of the Okazaki fragment being measured. $Flap_2$ corresponds to the length of DNA of the adjacent Okazaki fragment displaced by the mutant polymerase.

The second class of Okazaki fragments analyzed were completed fragments present on the long rolling circle tails in reactions employing the D219A polymerase. Here we could distinguish the fragment junctions by the presence of SSB stained flaps (Figures 3A–3C and Figure 4B). These fragments are defined as beginning with the displaced ssDNA, continuing toward the distal end of the tail through the duplex segment, and ending at the point where the polymerase started to displace the adjacent Okazaki fragment (Figure 4B). The length of the completed Okazaki fragment, therefore, is the length of the flap 5′ to the duplex region, $flap_1$, plus the duplex region minus the length of the flap 3′ to the duplex region, $flap_2$. The length of $flap_1$ must be added, since this flap was the result of the 5′ region of the Okazaki fragment having been displaced (had the D219A polymerase not strand displaced, the 5′ flap would have been part of the duplex segment). Conversely, $flap_2$ was

Table 1. Strings of Okazaki Fragment Lengths from Individual Replicating Molecules (64 nM Primase)

	Okazaki Fragment Number																								
Molecule Number	1	2	3	4	5	6	7	8	9	10	11	12	13	14	15	16	17	18	19	20	21	22	23	24	25
1	1.1	2.5	0.7	1.1	6.0	2.2	1.9	1.5	0.8	2.1	0.6	0.4	1.6												
2	1.6	1.2	3.4	3.4	6.8	1.4	4.1	3.5	2.6	1.3	1.2	2.0	1.8	2.7	4.4										
3	1.7	0.8	4.8	3.2	2.3	2.5	1.6	0.7	5.4	0.9															
4	0.9	2.3	1.2	1.6	1.7	1.0	2.4	4.2	2.0	8.2	0.3	1.9	3.1	2.2											
5	1.3	0.8	4.8	5.9	5.6	0.5																			
6	1.7	0.8	0.8	1.4	0.3	2.0																			
7	4.0	1.3	3.9	1.9	0.3	1.3	0.6	1.9	1.4																
8	1.5	1.0	2.9	1.9	2.2	2.0	2.9	1.9	0.9	2.3	1.3	6.3	1.2	1.1	0.6	1.3	3.9	0.6	3.3	1.2	1.9	1.8	2.9	0.8	4.6
9	2.0	3.1	1.8	4.4	0.8	2.8	0.6	1.5	1.2	3.9	3.4	1.7	7.1	0.8	2.4	4.1	1.3	2.7	0.5	1.2	3.7				
10	0.3	4.0	0.4	3.3	2.5	4.8	4.0	1.0	3.3	2.3	1.4	4.6	0.2	0.9	2.4	0.4	0.4								
11	3.1	0.9	0.6	2.3	2.6	0.4	3.2	1.0	0.7	1.1															
12	2.9	3.5	2.2	0.9	0.6	0.8	0.3	1.6	1.0	0.1	2.5	1.4													
13	1.2	2.3	3.0	3.1	3.3	3.6	1.4	2.2																	
14	0.8	2.0	1.6	2.4	1.2	3.0																			
15	0.5	0.5	1.0	1.1	1.5	2.7	3.2	2.7																	
16	1.0	0.7	1.1	3.6	0.8	5.0	1.4	2.5																	
17	0.8	1.5	1.4	1.5	1.8	1.7	1.1	0.4	2.6																
18	4.0	3.0	3.8	3.4	1.2	4.6	4.2	0.8	2.9	2.7	4.1	2.0	4.4												
19	2.3	3.9	3.7	0.2	3.6	2.9	3.2																		
20	0.9	2.9	2.2	4.5																					
21	0.7	1.7	0.9	7.5	0.2	1.7	3.2	1.4	1.6	1.7	3.1	0.9													
22	3.5	4.6	0.9	1.9	2.2	0.8	0.8	0.5	1.3	1.0	1.4														
23	4.8	3.7	1.2	1.9	3.5	1.9	2.6	1.4	1.4	2.7															
24	0.3	1.2	0.9	4.3	3.6	3.5	3.0																		

Rolling circle intermediates such as those in Figure 4 were photographed, and the lengths of successive individual fragments were determined using the criteria in Figure 4. Strings of values for 24 molecules replicated with 64 nM primase are shown. Okazaki fragment number 1 is the farthest from the template circle.
Results are shown in thousands of nucleotides.

generated by the D219A polymerase strand invading into the next Okazaki fragment. By subtracting the length of the $flap_2$ from the duplex length, one can account for the portion of the duplex length that is due to the strand displacement synthesis by the D219A polymerase.

If the distributions of Okazaki fragment lengths obtained by alkaline gel analysis and EM measurement are similar, this would strengthen our case for using this EM method to measure sequential fragment lengths along replicating molecules. Further, very long Okazaki fragments are observed by EM, and if the relative abundance of these long fragments is similar to that seen by gel analysis, this would argue that those detected by EM are not artifacts of having missed junctions between adjacent Okazaki fragments. The length histograms generated from the EM data present a number-weighted distribution with fragments of different lengths contributing equally. In contrast, the gel analyses are carried out by radiolabeling fragments uniformly and thus present a weight distribution with long fragments being weighted proportionately greater than short ones, and this difference must be accounted for. Finally, because the EM measurement provides the full fragment length, comparisons are best done using the D219 mutant polymerase, which will not degrade the 3′ termini of the Okazaki fragments.

To compare the EM and gel results, the distribution of fragment lengths from the gels (Figure 1B) were reduced to histograms. Each of the sample lanes on an alkaline gel containing size markers or DNA fragments from a reaction catalyzed by the D219 mutant polymerase and 64 nM primase (in the absence of RNase H and DNA ligase) was scanned using ImageQuant Software (see Experimental Procedures), and the relative intensities were determined. These raw profiles contain contributions from three populations: the full-length linear DNA (7200 nt) from leading strands that did not begin rolling circle synthesis, leading strand products (almost all $>$20,000 nt), and Okazaki fragments on the lagging strand. PeakFit software (see Experimental Procedures) was used to remove the contributions from the leading strand products and unit length linear DNAs. The resulting distributions were converted to lengths in nt based on the standards. The relative intensities of Okazaki fragments from 600 to 9000 nt were summed at 600 nt increments, and the distributions were converted to ones in which each fragment contributes equally, independent of its length. Finally, the histograms were approximated by a logarithmic normal function and plotted normalized to 100% of the total fragments (Figures 1C and 1D).

From the experiments described below with 64 nM primase, 261 Okazaki fragment lengths were collected from 24 different replicating molecules. These values were plotted using the same logarithmic normal function as above and compared with the fragment size distribution in gels (Figure 1C). The EM and gel profiles are very similar, with both showing some fragments as short as 400 nt and a few as long as 6000 nt (2% by EM and 1% by gel analysis). Both distributions peak between 1500 and 2200 nt. For comparison, a replication reaction was carried out using 64 nM primase and wild-type T4 polymerase (in the absence of RNase H and DNA ligase), and the products were displayed on an alkaline gel. EM analysis was carried out on 78 molecules undergoing

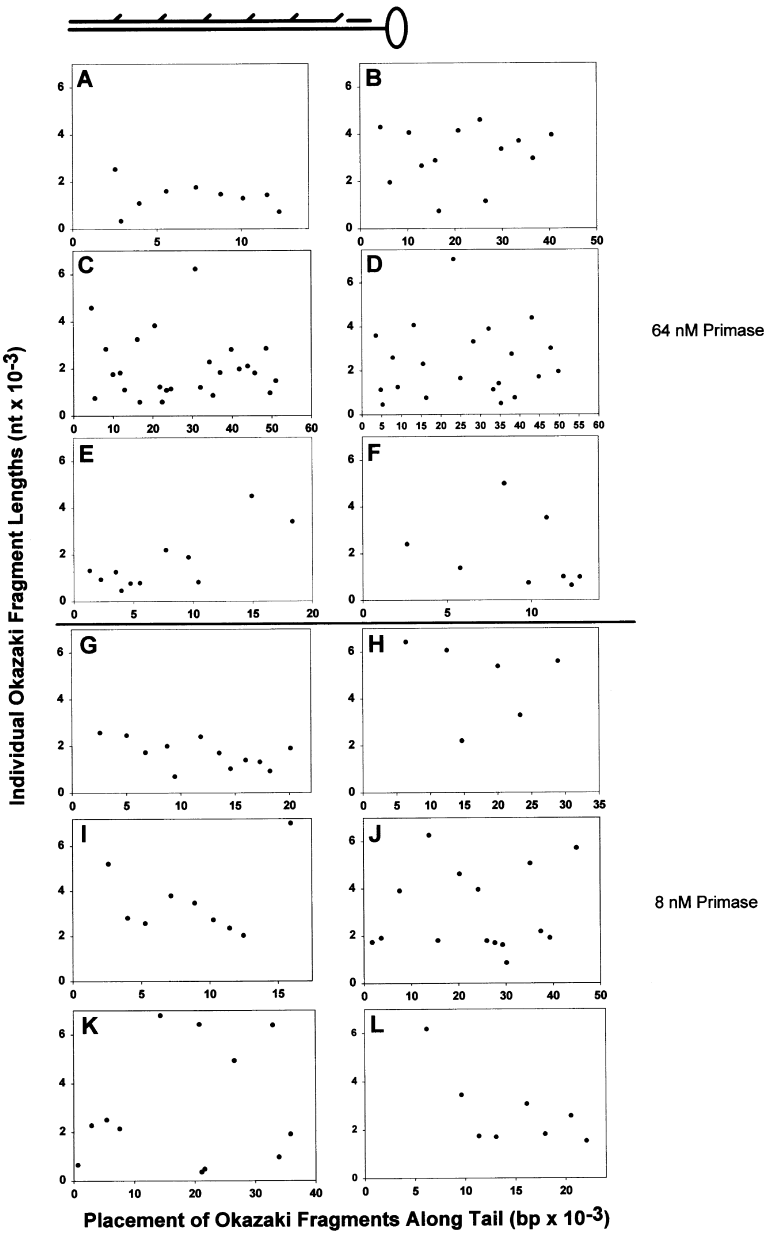

Figure 5. Sequential Okazaki Fragment Maps from Long Rolling Circle Replication Products

From micrographs such as those in Figure 3 and the measurement criteria described in Figure 4, the lengths of successive Okazaki fragments present along rolling circle tails generated by the D219A DNA polymerase in the absence of RNase H and ligase were determined. The length of each fragment is shown in the y axis, and the cumulative distance from the end of the DNA distal to the circular template is shown in the x axis. The orientation is shown in the illustration. Examples of fragment distributions synthesized in the presence of 64 nM (A–F) or 8 nM (G–L) primase.

replication under the same conditions but with RNase H and DNA ligase present. In this case, the nascent Okazaki fragments at the fork as measured by EM are being compared to the full distribution of fragments along the replicating tail in the gel analysis. Data reduction was done as above. As shown in Figure 1D, the two histograms are very similar, with the one from alkaline gel analysis shifted slightly to shorter sizes as expected due to some digestion by the exonuclease activity of the wild type polymerase. The excellent correlation between the two approaches provides a firm basis for using this EM mapping technique to determine the fragment distributions along single replicating molecules.

Okazaki Fragment Distributions under Optimal Replication Conditions

Under optimal conditions for rolling circle synthesis with the primed M13 ssDNA template as determined by total nucleotide incorporation and fragment size distribution, primase is present at 64 nM (Figure 1B, right; and data not shown). We generated a large number of rolling circle intermediates under these conditions using the D219A polymerase, and the ssDNA flaps at the junctions between Okazaki fragments were stained with SSB. Twenty-four such molecules were selected for detailed analysis based only on our ability to unambiguously trace the path of the tail from beginning to end (Table 1). The number of Okazaki fragments per molecule ranged from 4–25, with an average of 11. The smallest Okazaki fragment measured was 93 nt, and the largest Okazaki fragment measured was 8173 nt, with an average of 2002 nt.

To provide a graphic representation of these values on individual molecules, the length of each fragment was plotted in relation to its placement along the replication tail. The first data point (fragment length) represents

Table 2. Strings of Okazaki Fragment Lengths from Individual Replicating Molecules (8 nM Primase)

	Okazaki Fragment Number														
Molecule Number	1	2	3	4	5	6	7	8	9	10	11	12	13	14	15
1	5.2	1.0	1.4	2.7	2.2	2.8	3.9	0.7	2.7	4.2	1.0	5.1	4.7	3.6	
2	1.6	2.6	1.9	3.1	1.8	1.8	3.5	6.2							
3	4.2	3.6													
4	1.8	1.0	2.4	0.8	3.7	3.7	2.7	2.5	5.3						
5	1.9	1.1	4.0	1.3	2.1	3.7	0.4	4.6	0.6	2.6					
6	1.9	1.1	1.6	1.2	1.9	0.1	2.8	0.7	2.0	1.7	2.5	2.4	2.2		
7	1.9	2.3	0.8	3.3											
8	2.2	4.1	1.3	4.2											
9	0.7	2.9	0.6	4.2											
10	2.0	1.0	6.4	5.0	0.5	0.4	6.5	6.8	2.2	2.6	2.3	0.7			
11	1.0	4.3	0.4	7.2	2.3	0.4	5.2								
12	1.3	4.1	1.3	1.5	1.6	5.3	5.0	2.2							
13	3.8	2.6	1.5	1.2	4.7	0.3	0.6	3.2							
14	1.9	3.7	4.5	4.8	1.1	1.2	4.5	0.2	0.2	4.2					
15	3.9	3.9	9.3	0.7	7.0	5.6									
16	1.6	7.0	7.9	1.2	3.1	3.0									
17	1.9	1.0	2.5	5.4	7.1	1.1	6.1	0.6	0.8	2.1	3.8				
18	0.2	2.4	7.1	1.4	0.9	5.4									
19	8.3	0.9	1.8	2.4	1.6	5.9									
20	5.6	3.3	5.4	2.3	6.1	6.5									
21	1.6	0.5	5.4	1.6	6.0										
22	3.2	4.5	3.4	3.1	7.6	5.8	10.1	1.6							
23	1.3	2.6	2.0	1.9											
24	1.8	1.7	2.7	2.9	1.9	2.2									
25	7.0	2.1	2.4	2.8	3.5	3.8	2.6	2.9	5.3						
26	1.9	1.0	1.4	1.4	1.1	1.8	2.5	0.7	2.1	1.8	2.5	2.6			
27	1.7	3.0	2.6	3.4											
28	1.8	2.7	2.2												
29	10.6	3.6	4.8	6.9	1.7	3.5									
30	3.3	0.5	6.3												
31	5.8	2.0	2.2	5.1	0.9	1.7	1.8	1.8	4.0	4.7	1.8	6.3	4.0	2.0	1.8
32	2.0	2.0	3.0												

Rolling circle intermediates such as those in Figure 4 were photographed, and the lengths of successive individual fragments were determined using the criteria in Figure 4. Strings of values for 32 molecules replicated with 8 nM primase are shown.
Results are shown in thousands of nucleotides.

the first fragment synthesized and thus the one at the end of the DNA tail farthest from the rolling circle template (illustration, Figure 5, top). The Okazaki fragment lengths showed marked variations from one to the next along the replication tail. In some cases, the lengths gradually increased and decreased in size (Figure 5A), and in other cases the Okazaki fragment sizes fluctuated rapidly between large and small sizes (Figures 5B and 5C). Only when the Okazaki fragments gradually shifted from short to long lengths were multiple neighboring Okazaki fragments of similar size (Figure 5A). Molecules with long Okazaki fragments throughout the replication tail (Figure 5B) fluctuated more in size than molecules that had predominantly small Okazaki fragments (Figure 5A). This trend also held for molecules that contained regions of short Okazaki fragments followed by regions of large ones (Figure 5D) or vice versa (Figure 5E).

Okazaki Fragment Distributions under Conditions of Reduced Primase Concentration

From previous studies (Richardson et al., 1990; Wu et al., 1992a, 1992b, 1992c; Zechner et al., 1992a, 1992b; Park et al., 1998), we would expect some change in the average Okazaki fragment length if the concentration of primase was changed. Alkaline agarose gel analysis (Figure 1B, right) revealed that the Okazaki fragments were larger ($\sim$3000 nt average) when the incubations contained 8 nM primase as contrasted to 64 nM primase (with all other protein concentrations remaining unchanged).

We analyzed the Okazaki fragment lengths (n = 232) from 32 molecules derived from reactions with 8 nM primase (Figure 3C and Table 2). The number of Okazaki fragments per molecule ranged from 2–13, with an average number of 7. The smallest Okazaki fragment measured was 83 nt, and the largest was 10,500 nt. The average length of 2910 nt was $\sim$900 nt greater than the size of the Okazaki fragments under optimum conditions (64 nm primase). These values agree well with the alkaline agarose gel data (Figure 1B). When the pattern of fragment length variations was plotted for representative molecules, the lengths of individual Okazaki fragments showed similar profiles to those observed with 64 nM primase (Figures 5G–5L).

Comparison of Multiple Okazaki Fragment Strings with the Total Fragment Population

From these data, there were sufficient examples to provide a comparison between individual replicating molecules and the total population average. This comparison directly addresses the question posed (see Introduction) as to whether the broad population distribution is due to

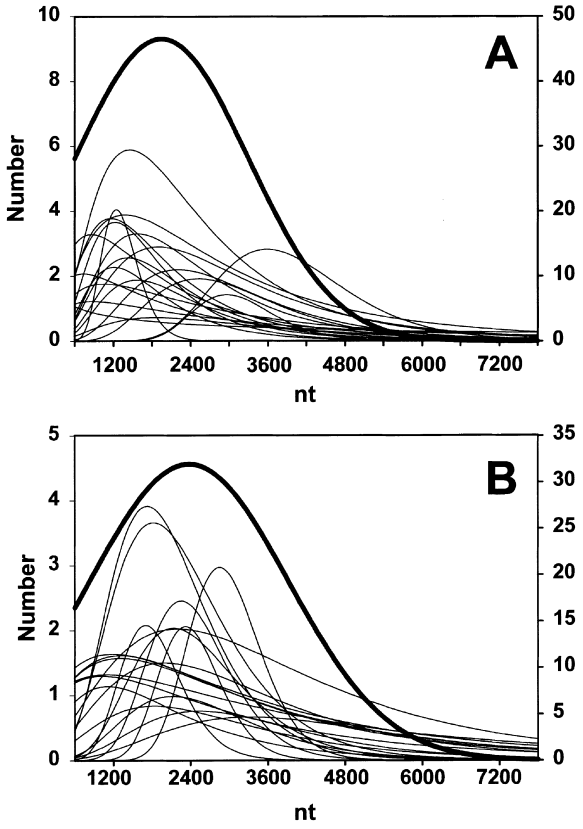

Figure 6. Comparisons of Okazaki Fragment Distributions from Single Replicating Molecules with that of the Total Population

Okazaki fragment lengths along single replicating molecules taken from Tables 1 and 2 (A and B, respectively) were plotted as smoothed log normal distributions (thin lines; y axis values on left) and are compared to the total population of Okazaki fragment lengths plotted similarly (thick line; y axis values on right). Reactions are with 64 nM (A) and 8 nM (B) primase.

a series of single molecule distributions, each of which is narrow but centering about a different mean, or whether the individual molecule distributions would be as broad as that of the total population of fragments. Individual strings of Okazaki fragments from 8 and 64 nM primase were plotted as smoothed histograms and overlaid as shown in Figure 6 along with a smoothed histogram representing the pool of all of the fragments. From these results, it is clear that the individual distributions in most cases span nearly as broad a range as that of the full population.

Discussion

In this paper, we present a study in which the lengths of individual, sequential Okazaki fragments have been mapped along single replicating DNA molecules. These data are of central importance for advancing our understanding of how Okazaki fragments are initiated. While the individual data themselves do not prove any one particular model of Okazaki fragment synthesis, they impose constraints on all models and will help direct further experiments and model development. This study was possible due to the properties of an exonuclease mutant of T4 DNA polymerase that displaces a short DNA segment at the junction of two Okazaki fragments, generating a "flag" which can be detected by EM. Comparisons of reactions of the wild-type and mutant polymerases showed no significant differences in the synthesis reactions other than the generation of these short flaps.

The distribution of Okazaki fragment lengths measured by EM compared very well with that derived from alkaline gel analysis. Further, the moderate increase in size noted in alkaline gels when the primase concentration was reduced was also reflected in the mean fragment size determined by microscopy. The resolution of the EM method in these experiments would be the minimal distance between two very closely spaced Okazaki fragments that could be detected. We estimate this to be on the order of $\sim$150 bp, which is significantly shorter than the length of the smallest Okazaki fragment expected based on alkaline gel analysis. Thus, we have confidence that the EM mapping method has provided a representative picture of the Okazaki fragment distributions along the replicating DNAs.

Inspection of the data for two different concentrations of primase revealed that the distribution of fragment lengths along single molecules was nearly as broad as that found for the total population with fragments as short as 500 nt and some as long as 5000 nt. There were no obvious trends, such as fragment lengths being highly variable at the outset and then becoming more similar in size, or fragment lengths initially being short and then gradually increasing in length. The full data set has been presented here (Table 1) so that others who might wish to examine the data using approaches such as the analysis of Markov chains could do so. It is worth noting that the distributions seen by both gel analysis and EM are not Gaussian but rather rise sharply and then tail off more gradually.

While selected molecules could be found in which runs of similar length fragments were present (five or more with lengths within 20% of each other), such molecules were rare, representing less than 10% of the total. It might be argued that only for these rare molecules was the replication machinery properly assembled and that these (rare) examples were present in a high background of molecules in which the replisomes were not fully assembled. Were this the case, we would have expected to see chains of similar-sized fragments more frequently along the very long replicating tails where there had been sufficient time to achieve a highly coordinated state. In fact, this was never the case, and chains of similar sized fragments were found on DNAs with relatively short tails. Further, upon variation of the polymerase concentration severalfold and primase concentration over an 8-fold range, the fraction of molecules with similar sized chains remained below 10%. Finally, the reaction conditions with 64 nM primase represent the result of detailed biochemical optimization of the replication conditions and factors, and $>$2/3 of the duplex M13 circles examined had long rolling circle tails with no gaps (when DNA ligase and RNase H were included), indicating a highly coupled reaction. Thus, we conclude that the relatively broad distribution observed within individual molecules directly maps to a similar broad distribution for the population.

In the model proposed by Selik et al. (1987) based on the T4 system, it was suggested that it may require synthesis of up to eight Okazaki fragments for the replisome to establish and "lock onto" a stable Okazaki fragment length. If so, we might have observed high variability in fragment length over the first eight Okazaki fragments at the 5′ end of the replication tail, followed by fragments of similar size. No such examples were seen. The results presented here are also not in concert with the primase control model (Tougu and Marians, 1996) where the availability of primase and its ability to interact with the helicase at the fork for primer synthesis controls the cycle. While both our EM and alkaline gel analysis confirmed the larger average fragment size at lower primase concentration predicted by the primase control model, the EM analysis showed that the distribution of fragments sizes along single molecules was equally broad at low and optimal primase concentration.

In the collision models, initiation of a new Okazaki fragment is controlled by a single interaction within the replicating complex, between the lagging strand polymerase and the 5′ terminus of the previous Okazaki fragment. Similarly, in the primase control models, initiation is controlled by the binding or release of the primase. These events, however, occur within a large replisome that contains many proteins and subassemblies. *E. coli* primase, bound to SSB, remains tightly associated with the newly synthesized primer. To load the β clamp on the primer, the χ subunit of the *E. coli* clamp loader first binds SSB, which leads to the release of the primase by decreasing the SSB–primase interaction (Yuzhakov et al., 1999a). A similar switch between the primase and clamp loader on SSB has been shown with eukaryotic replication proteins (Yuzhakov et al., 1999b).

Primase, polymerase, and rNTP are required to begin a new Okazaki fragment, and, as reviewed above, changing the concentration of any of these factors can change the average length of fragments in a replication reaction. However, even when the concentrations of these three components are held constant, we find great variation in the distribution of fragment sizes on individual molecules of identical sequence. Recent electron microscopic analysis of replicating molecules suggests that the structure of the ssDNA in the lagging strand loop at the replication fork may be an additional factor affecting the start of a new fragment. EM examination has revealed lagging strand loops in the T7 system (Lee et al., 1998; Park et al., 1998), and more recently in the T4 (these authors, submitted) and in the *E. coli* systems (unpublished observations, Griffith, Marians, and McHenry laboratories). In all three cases, very similar structures are present consisting of a compact replisome, a loop that is double stranded, and two single-stranded segments (on the lagging strand) that are highly compacted and part of the replisome complex. It is likely that the structure of the ssDNA is a consequence of its tight association with SSB proteins.

At the start of each fragment, primase must bind to a rapidly moving helicase when it is close to a primase recognition sequence, and the clamp and polymerase must assemble on the new primer. During each round of Okazaki synthesis, there may be strong torsional constraints generated, as the trombone loop grows and becomes increasingly bulky as the DNA strands are threaded through the replisome. If so, then the fraction of time that a primase recognition site is accessible to primase and the newly synthesized primer is also accessible to the clamp loader may initially be very small and then progressively increase through a single trombone cycle. This could lead to a complex distribution of fragment start sites on individual molecules. The fact that very similar average size distributions are seen in the T7 system when the template is reduced 100-fold in size (Lee et al., 1998) could, by this model, be explained by the observation that on both the large and small template circles the same sized lagging strand loops are generated, and the replication complex remains the same. If this model is valid, determination of the architecture of the DNA strands and protein complexes at the replication fork will be necessary to further understand the control of the lagging strand cycle.

Experimental Procedures

Reagents and Enzymes

Unlabeled nucleoside triphosphates and T4 DNA ligase were obtained from Pharmacia Biotech Inc., and [α-^{32}P]dCTP and dTTP were obtained from Dupont NEN Inc. The bacteriophage T4 gene 32 ssDNA binding protein, 41 helicase, 43 DNA polymerase, 44/62 clamp-loader, 45 clamp, 59 helicase loading protein, 61 primase, and RNase H proteins were purified to homogeneity as described elsewhere (Nossal et al., 1995). All proteins were free of detectable endonuclease activity. *E. coli* SSB protein was prepared according to Chase and Williams (1986).

DNA Synthesis

The primer-template used was made by annealing an 84-base oligonucleotide, complementary to positions 6198–6281 of M13mp19, to M13mp2 ssDNA. When annealed, only the 3′ 34 nt are complementary, leaving a 50 nt unpaired tail. The reaction mixtures (10 μl) contained 16 fmol (circular molecules) of the primer-template, 2 mM ATP, 250 μM of each dNTP including [α-^{32}P]dCTP or dTTP, (approximately 800 cpm/pmol), 250 μM CTP, GTP, and UTP, 25 mM K HEPES (pH 7.6), 60 mM potassium acetate, 6 mM magnesium acetate, 10 mM β-mercaptoethanol, and 20 μg/ml bovine serum albumin. Enzymes were diluted in a solution containing 50 mM K HEPES (pH 7.6), 100 mM KCl, 5 mM $MgCl_2$, 1 mM EDTA, 10 mM β-mercaptoethanol, 100 μg/ml bovine serum albumin, and 25% glycerol. Unless otherwise noted, the protein concentrations were 2 μM gene 32 ssDNA binding protein, 328 nM gene 41 helicase, 30 nM wild-type or exonuclease-defective D219A (Frey et al., 1993) DNA polymerase, 242 nM genes 44/62 clamp-loader, 162 nM gene 45 clamp, 95 nM gene 59 helicase loading protein, and 8 or 64 nM gene 61 primase. When indicated, RNase H was 195 nM, and DNA ligase was 75 Weiss units/ml. Reaction mixtures without polymerase, primase, helicase, RNase H, and DNA ligase were incubated for 2 min at 37°C, and synthesis was begun by the addition of a mixture of these proteins. At 2 and 5 min, aliquots of the reaction mixtures were mixed with an equal volume of 0.2 M EDTA to stop the synthesis, and the products were analyzed by alkaline agarose gel electrophoresis. For EM, identical reactions were incubated and stopped as above, and the reaction volume was increased to 100 μl by the addition of SDS to 1% and protease K to 1 mg/ml. After incubating the samples for 1 hr at 37°C, the samples were chromatographed through 2 ml Biogel A5M (Bio-Rad Inc.) columns to remove the denatured and proteolyzed proteins.

Alkaline Agarose Gel Electrophoresis

Alkaline electrophoresis loading buffer was added to the stopped reactions to produce a final concentration of 67 mM NaOH, 17% glycerol, and 0.03% w/v bromocresol green. The radioactive DNA products were analyzed by electrophoresis through 0.6% alkaline agarose gels in 30 mM NaOH and 2 mM EDTA. The dried gels were autoradiographed without an intensifying screen. The sizes of the

radioactively labeled DNA strands were determined by comparison with 3′ end-labeled ^{32}P λ DNA HindIII restriction fragments.

Length Distribution of Okazaki Fragments in Alkaline Gels

Alkaline gels of Okazaki fragments and markers were scanned using ImageQuant software (Molecular Dynamics). The apparent sizes in nt of the Okazaki fragments in the gels were determined from a calibration curve generated from a plot of the log of the length of the fragment versus the distance migrated using λ HindIII fragments ranging from 0.6 to 9.4 kb. This calibration curve was used to translate migration distance (in pixels) to length (in nt).

PeakFit software (SPSS Inc.) was used to extract the contribution due to Okazaki fragments in the alkaline gels from the leading strand products during rolling circle synthesis and the 7.2 kb template molecules where polymerase stalled after copying the single-stranded template. The curve from the gel analysis was broken into a set of separate log normal curves whose individual parameters were varied until the sum of the set generated a good approximation of the initial curve. These curves were further processed including approximation by logarithmic normal function (see Results). Finally the curves were reduced to ones in which each fragment contributes equally, independent of its length. All distributions including the EM data were normalized to 100%, and histograms were created using SigmaPlot software (SPSS Inc.).

Electron Microscopy

To examine the products of the replication reactions, incubation reactions described above were stopped and deproteinized as described above. *E. coli* SSB protein was then added to 1 μg/ml on ice for 5 min and then fixed in place with 0.6% glutaraldehyde for 5 min. The samples were adsorbed to thin carbon supports in the presence of spermidine, washed, air dried, and rotary shadowcast with tungsten (Griffith and Christiansen, 1978). Samples were examined in a Phillips CM12 instrument at 40 kV. Length measurements were either made by projecting images on the micrographs onto a Summagraphics digitizing tablet coupled to a MacIntosh Quadra 650 computer programmed with software developed by J. D. G., or by capturing the electron microscope images with a Gatan 724 slow scan CCD camera and then using Digital Micrograph 3.3 (Gatan Inc.).

Acknowledgments

This work was supported by grants from the National Institutes of Health to J. D. G. (GM31819, CA19014, and CA70343) and from the NIDDK intramural program to N. G. N.

Received July 11, 2000; revised August 22, 2000.

References

Alberts, B.M., Barry, J., Bedinger, P., Formosa, T., Jongeneel, C.V., and Kruezer, K.N. (1983). Studies on DNA replication in the Bacteriophage T4 in vitro system. Cold Spring Harbor Symp. Quant. Biol. *47*, 655–668.

Chase, J.W., and Williams, K.R. (1986). Single-stranded DNA binding proteins required for DNA replication. Annu. Rev. Biochem. *55*, 103–136.

Debyser, Z., Tabor, S., and Richardson, C.C. (1994). Coordination of leading and lagging strand DNA synthesis at the replication fork of bacteriophage T7. Cell *77*, 157–166.

Frey, M.W., Nossal, N.G., Capson, T.L., and Benkovic, S.J. (1993). Construction and characterization of a bacteriophage T4 DNA polymerase deficient in 3′ to 5′ exonuclease activity. Proc. Natl. Acad. Sci. USA *90*, 2579–2583.

Griffith, J., and Christiansen, G. (1978). Electron microscope visualization of chromatin and other DNA-protein complexes. Annu. Rev. Biophys. Bioeng. *7*, 19–35.

Hacker, K.J., and Alberts, B.M. (1994). The rapid dissociation of the T4 DNA polymerase holoenzyme when stopped by a DNA hairpin helix. A model for polymerase release following the termination of each Okazaki fragment. J. Biol. Chem. *269*, 24221–24228.

Hollingsworth, H.C., and Nossal, N.G. (1991). Bacteriophage T4 encodes an RNase H which removes RNA primers made by the T4 replication system in vitro. J. Biol. Chem. *266*, 1888–1897.

Hinton, D.M., and Nossal, N.G. (1987). Bacteriophage T4 DNA primase-helicase. Characterization of oligomer synthesis by T4 61 protein alone and in conjunction with T4 41 protein. J. Biol. Chem. *262*, 10873–10878.

Kornberg, A., and Baker, T. (1992). DNA Replication, Second Edition (New York: W. H. Freeman).

Lee, J., Chastain, P.D., Kusakabe, T., Griffith, J.D., and Richardson, C.C. (1998). Coordinated leading and lagging strand DNA synthesis on a minicircular template. Mol. Cell *1*, 10001–11010.

Nossal, N.G. (1994). The bacteriophage T4 DNA replication fork. In Molecular Biology of Bacteriophage T4, J. Karem, ed. (Washington, D.C.: American Society for Microbiology), pp. 43–52.

Nossal, N., and Alberts, B.M. (1983). Mechanism of DNA replication catalyzed by purified T4 DNA replication proteins. In Bacteriophage T4, C.K. Matthews, E.M. Kutter, G. Mosig and P.B. Berget, eds. (Washington, D.C.: American Society for Microbiology), pp. 71–81.

Nossal, N.G., Hinton, D.M., Hobbs, L.J., and Spacciapoli, P. (1995). Purification of the bacteriophage T4 DNA replication proteins. Methods Enzymol. *262*, 560–584.

Park, K., Debyser, Z., Tabor, S., Richardson, C.C., and Griffith, J.D. (1998). Formation of a DNA loop at the replication fork generated by bacteriophage T7 replication proteins. J. Biol. Chem. *273*, 5260–5270.

Richardson, R.W., and Nossal, N.G. (1989). Trypsin cleavage in the COOH terminus of the bacteriophage T4 gene 41 DNA helicase alters the primase-helicase activities of the T4 replication complex in vitro. J. Biol. Chem. *264*, 4732–4739.

Richardson, R.W., Ellis, R.L., and Nossal, N.G. (1990). Protein-protein interactions within the bacteriophage T4 DNA replication complex. Molecular mechanisms in DNA replication and recombination. UCLA Symp. Mol. Cell. Biol. *127*, 247–259.

Salinas, F., and Benkovic, S.J. (2000). Characterization of bacteriophage T4-coordinated leading and lagging strand synthesis on a minicircle substrate. Proc. Natl. Acad. Sci. USA *97*, 7196–7201.

Selik, H.E., Barry, J., and Cha, T.-A., Munn, M., Nakanishi, M., Wong, M.L., and Alberts, B.M. (1987). Studies on the T4 Bacteriophage DNA replication system. DNA replication and recombination. UCLA Symp. Mol. Cell. Biol. *47*, 183–214.

Sinha, N., Morris, C., and Alberts, B. (1980). Efficient in vitro replication of double stranded DNA templated by a purified T4 bacteriophage replication system. J. Biol. Chem. *255*, 4290–4303.

Stukenberg, P.T., Turner, T., and O'Donnell, M. (1994). An explanation for lagging strand replication: polymerase hopping among sliding clamps. Cell *78*, 877–887.

Tougu, K., and Marians, K.J. (1996). The interaction between helicase and primase sets the replication fork clock. J. Biol. Chem. *271*, 21398–21405.

Wu, C., Zechner, E.L., and Marians, K.J. (1992a). Coordinated leading and lagging strand synthesis at the Escherichia DNA replication fork: I. Multiple effectors act to modulate Okazaki fragment size. J. Biol. Chem. *267*, 4030–4044.

Wu, C., Zechner, E.L., Reems, J., McHenry, C., and Marians, K.J. (1992b). Coordinated leading and lagging strand synthesis at the Escherichia DNA replication fork: V. Primase action regulates the cycle of Okazaki fragment synthesis. J. Biol. Chem. *267*, 1074–1083.

Wu, C.A., Zechner, E.L., Hughes, A.J., Frandon, M.A., McHenry, C.S., and Marians, K.J. (1992c). Coordinated leading and lagging strand synthesis at the Escherichia DNA replication fork: IV. Recognition of an asymmetric dimeric DNA polymerase III holoenzyme. J. Biol. Chem. *267*, 4064–4073.

Yuzhakov, A., Turner, J., and O'Donnell, M. (1996). Replisome assembly reveals the basis for asymmetric function in leading and lagging strand replication. Cell *86*, 877–886.

Yuzhakov, A., Kelman, Z., and O'Donnell, M. (1999a). Trading places on DNA—a three-point switch underlies primer handoff from primase to the replicative DNA polymerase. Cell *96*, 153–163.

Yuzhakov, A., Kelman, Z., Hurwitz, J., and O'Donnell, M. (1999b). Multiple competition reactions for RPA order the assembly of the DNA polymerases delta holoenzyme. EMBO J. *18*, 6189–6199.

Zechner, E.L., Wu, C., and Marians, K.J. (1992a). Coordinated leading and lagging strand synthesis at the Escherichia DNA replication fork: II. Frequency of primer synthesis and efficiency of primer utilization controls Okazaki fragment size. J. Biol. Chem. *267*, 4045–4053.

Zechner, E.L., Wu, C.A., and Marians, K.J. (1992b). Coordinated leading and lagging strand synthesis at the Escherichia DNA replication fork: III. Polymerase-primase interaction governs primer size. J. Biol. Chem. *267*, 1054–1063.